An Overview (i.e. Promises and Perils) of the Phase-Field Approach for Fracture

Alain Karma
Northeastern University Boston

Collaborators:
Herbie Levine (UCSD)
Dave Kessler (Bar-Ilan)
Alex Lobkovsky (NU →MIT)
Vincent Hakim (ENS)

Acknowledgments: support of DOE and ENS Condorcet Chair in 2004.

August 19, 2005.

A piece of paper with a semicircular notch and a V shaped notch, and pulled. It failed at the point of the V, where the stress was greatest.

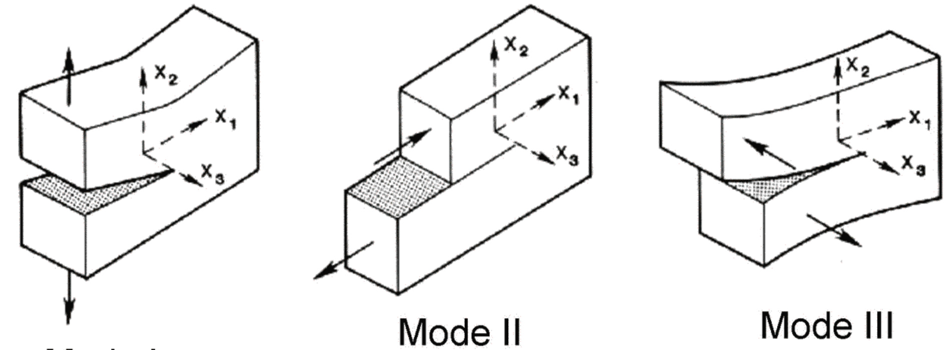

Mode I
"opening"

Mode II
In-plane shear
"sliding"

Mode III
Anti-plane shear
"tearing"

$$\sigma_{ij}^m(r,\theta) = \frac{K_m}{\sqrt{2\pi r}} f_{ij}^m(\theta)$$

$$G = \alpha(K_1^2 + K_2^2) + K_3^2/(2\mu)$$

$$\alpha \equiv (1-\nu^2)/E$$

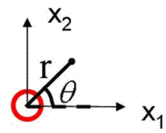

$$G = \Gamma(V)$$

Crack path prediction

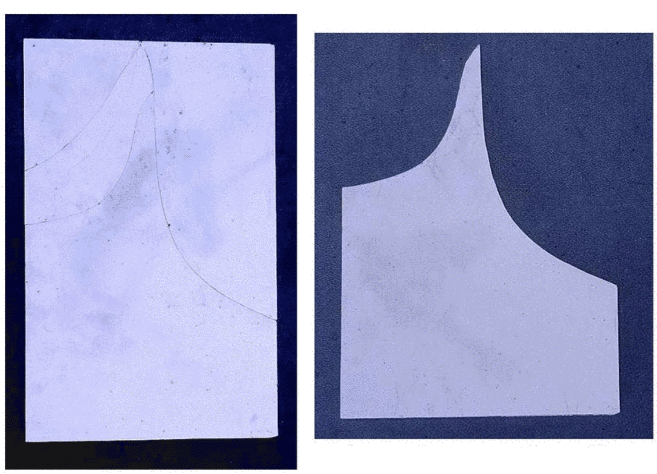

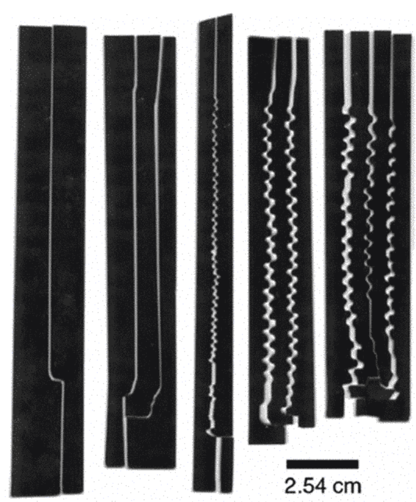

Silicon: Deegan et al. (2003)

Glass: Yuse and Sano (1993); Ronsin and Perrin (1997)

Crack path prediction for antiplane shear fracture (pure mode III)

G. I. Barenblatt and G. P. Cherepanov, PMM **25**, 1110 (1961) [J. Appl. Math. Mech. **25**, 1654 (1961)].

$$\sigma_{3\theta} \equiv \frac{\mu}{r}\frac{\partial u_3}{\partial \theta} = \frac{K_3}{\sqrt{2\pi r}}\cos\frac{\theta}{2} - \mu A_2 \sin\theta + \ldots$$

Principle of local symmetry: assumes propagation with symmetrical stress distribution about the crack axis:

$$A_2 = 0$$

Crack path prediction for plane loading

R. V. Goldstein and R. L. Salganik, Int. J. Fract. **10**, 507 (1974) and references therein.

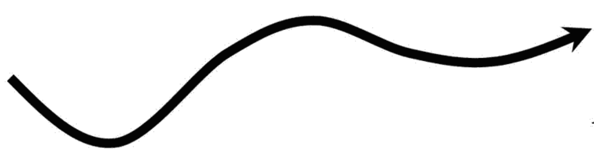

Local symmetry

$$K_{II} = 0$$

Assumes crack tip propagates in pure opening mode.

Implies that short scale dynamics of process zone has no influence on crack path

Is this always true and what is the generalization to anisotropic materials ?

Fracture surface of circularly cracked cylinder in pure torsion

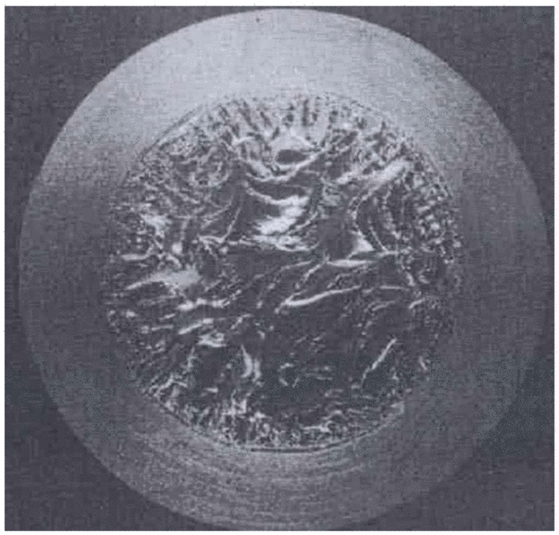

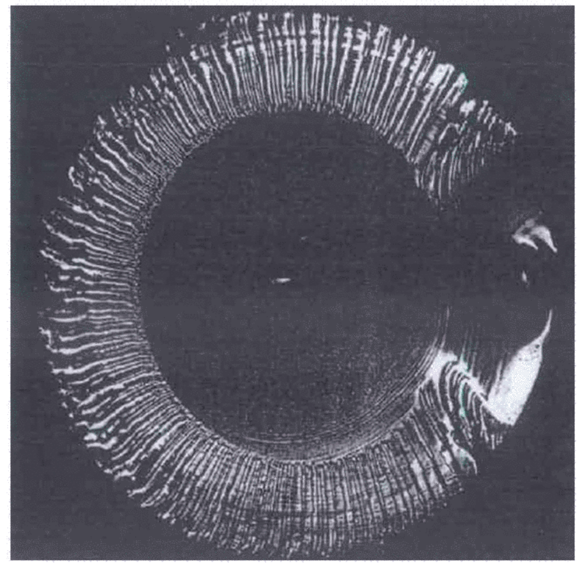

Sommer (1969)

Palaniswamy and Knauss

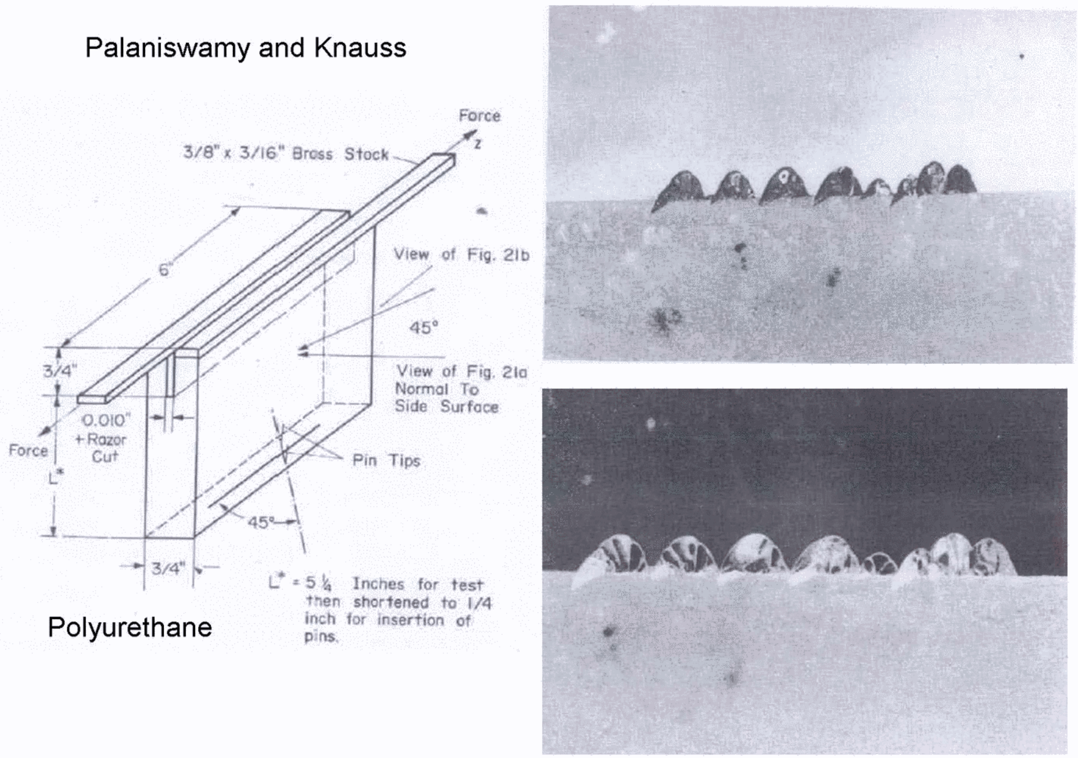

Polyurethane

Theoretical analyses:
Gao and Rice (1986)
Mochvan, Gao and Willis (1998)
Lazarus, Leblond and Mouchrif (2001)

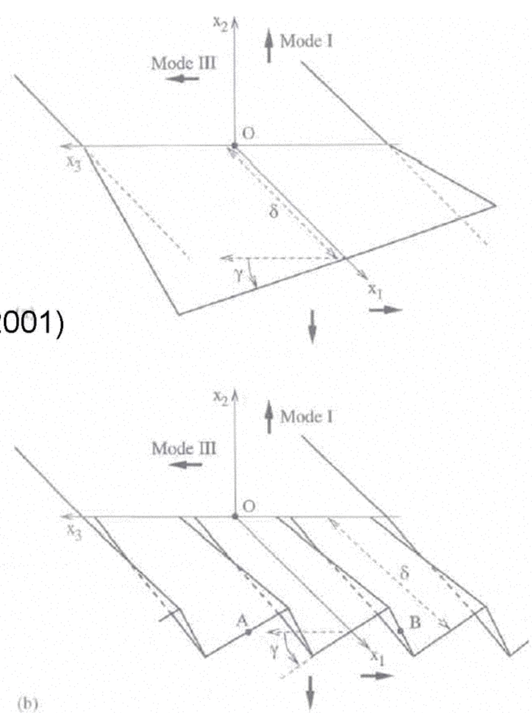

Dynamic instability

(Fineberg et al. 1991, Sharon & Fineberg, 1999, Livne *et al.* 2005)

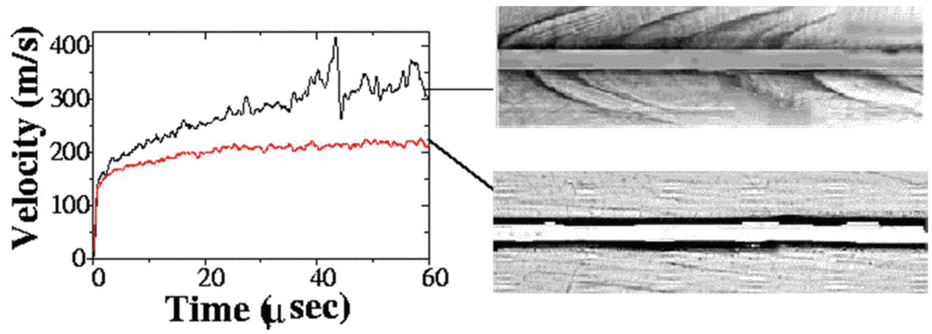

Apparent universality of micro-branching phenomenon suggests a possible continuum description but the role of the short-scale physics remains elusive.

"The Thermodynamic Theory of Capillarity Under the Hypothesis of a Continuous Variation of Density"

J. D. van der Waals

Amsterdam (1893); English trans. J.S. Robinson, J. Stat Phys (1979)

"*According to Gibbs' theory, capillary phenomena are present only if there is a discontinuity between the portions of fluid face-to-face…In contrast, the method that I propose in the following pages is not a satisfactory treatment unless the density of the body varies continuously at and near its transition layer.*"

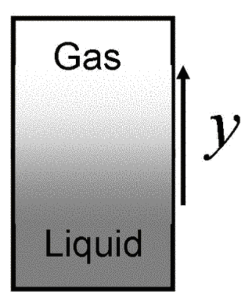

$$P_G - P_L = \frac{2\gamma}{R}$$

$$\gamma \sim \int \left(\frac{d\rho}{dy} \right)^2 dy$$

Historical Perspective

- van der Waals (1893)
- Ginzburg-Landau (1950)
- Cahn-Hilliard (1958)
- Critical phenomena (Halperin, Hohenberg and Ma,1974)
- Solidification (Langer,1978…1986; Collins and Levine, 1985)
- Outburst of activity has lead to the extension of the phase-field approach to a large number of interfacial pattern formation problems over the last two decades.

Phase-Field Model for Solidification

(Langer, 78-86; Collins-Levine, 85)

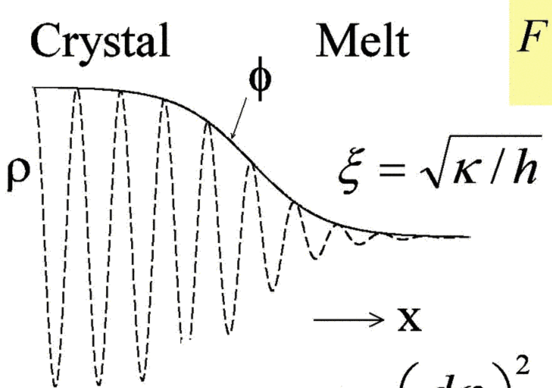

$$F = \int dV \left[\frac{\kappa}{2} |\vec{\nabla}\varphi|^2 + f_{DW}(\varphi) \right]$$

$$\xi = \sqrt{\kappa / h}$$

$$\gamma = \xi h \int dy \left(\frac{d\varphi}{dy} \right)^2$$

Double-Well Potential

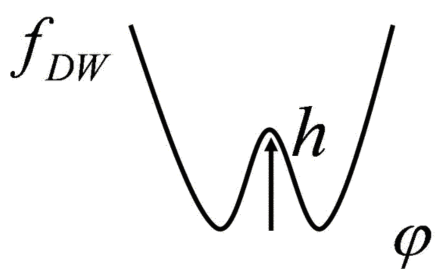

The terminology "phase-field" originates from the role of the order parameter φ in distinguishing between solid and liquid.

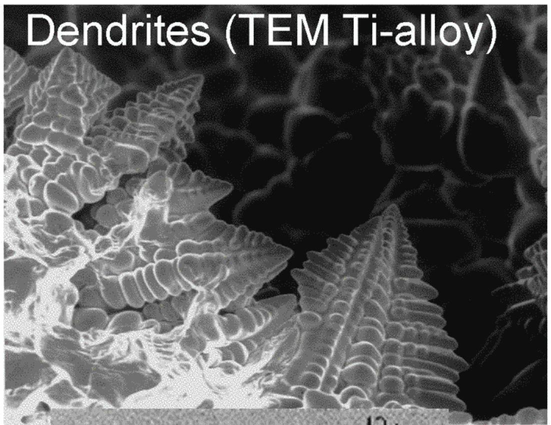

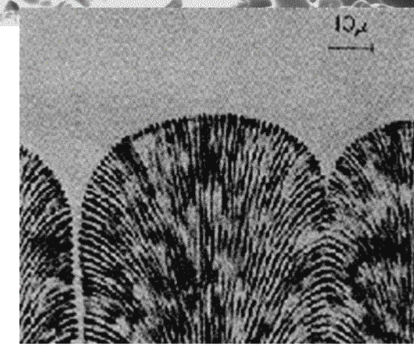

J. Bragard, A. Karma, Y. H. Lee, and M. Plapp, *Interface Science* **10**, 121-136 (2002).

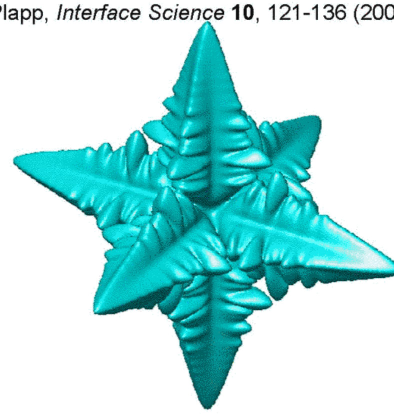

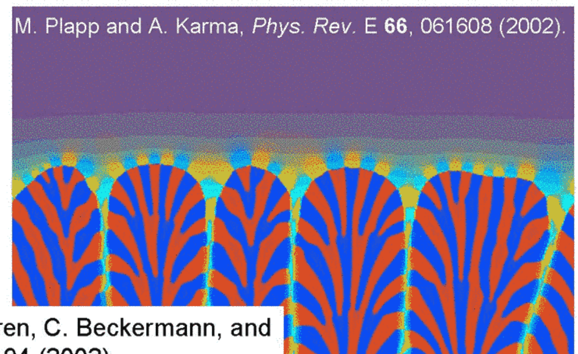

M. Plapp and A. Karma, *Phys. Rev.* E **66**, 061608 (2002).

Recent review: W. J. Boettinger, J. A. Warren, C. Beckermann, and A. Karma, *Ann. Rev. Mater. Res.* **32**, 163-194 (2002).

Benchmark quantitative comparisons with sharp-interface calculations and experiments

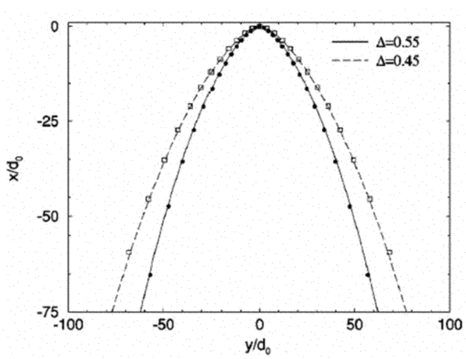

Comparison of phase-field simulations (solid and dashed lines) and Green's function solution of free-boundary problem (symbols). Karma and Rappel (1998).

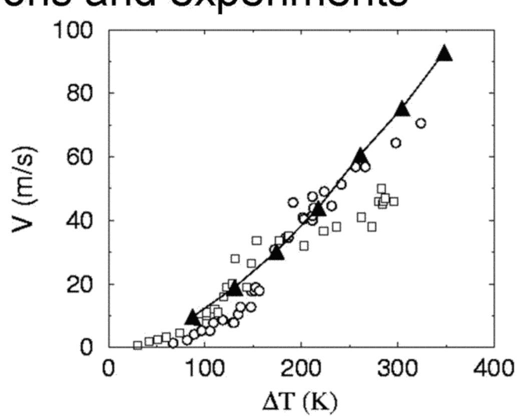

Comparison of phase-field simulations (solid line and triangles) and experiments (open symbols) for dendrite growth rate V in pure undercooled Ni. Bragard *et al.* (2002).

Applications (partial list)

- Solidification (dendrites, eutectics, etc)
- Solid-state phase transformations
- Grain growth
- Epitaxial growth
- Stress-induced instabilities (Grinfeld, etc)
- Dislocation dynamics
- Electrochemistry
- Corrosion
- Electromigration
- Hydrodynamic instabilities (Viscous fingering, etc)
- Fracture

Phase Field Modeling, A. Karma, in Handbook of Materials Modeling. Volume I: Methods and Models, edited by S. Yip, Springer, Netherlands, pp. 2087-2103 (2005).

Polycrystalline Materials

J.A. Warren, R. Kobayashi, A.E. Lobkovsky, and W.C. Carter, *Acta Mater.*, 51, 6035, 2003.

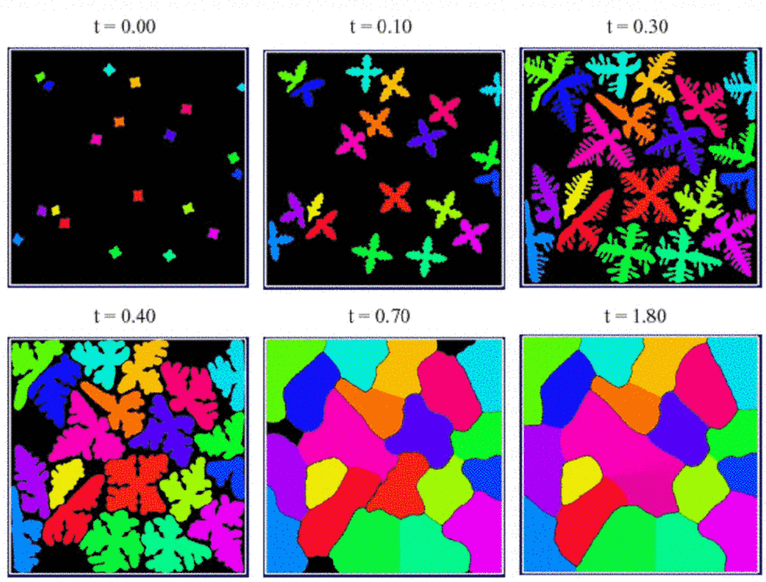

Phase-Field Models for Fracture

I. S. Aranson *et al.*, Phys. Rev. Lett. **85**, 118 (2000).

A. Karma, D. Kessler, and H. Levine, Phys. Rev. Lett. **87**, 045501 (2001).

L. O. Eastgate, J. P. Sethna, M. Rauscher, T. Cretegny, C.-S. Chen, and C. R. Myers, Phys. Rev. E 65, 036117 (2002).

Y. U. Wang, Y. M. Jin, and A. G. Khachaturyan J. Appl. Phys. **91**, 6435 (2002).

V. I. Marconi and E. A. Jagla, Phys. Rev. E **71**, 036110 (2005).

One-dimensional snap back of elastic band

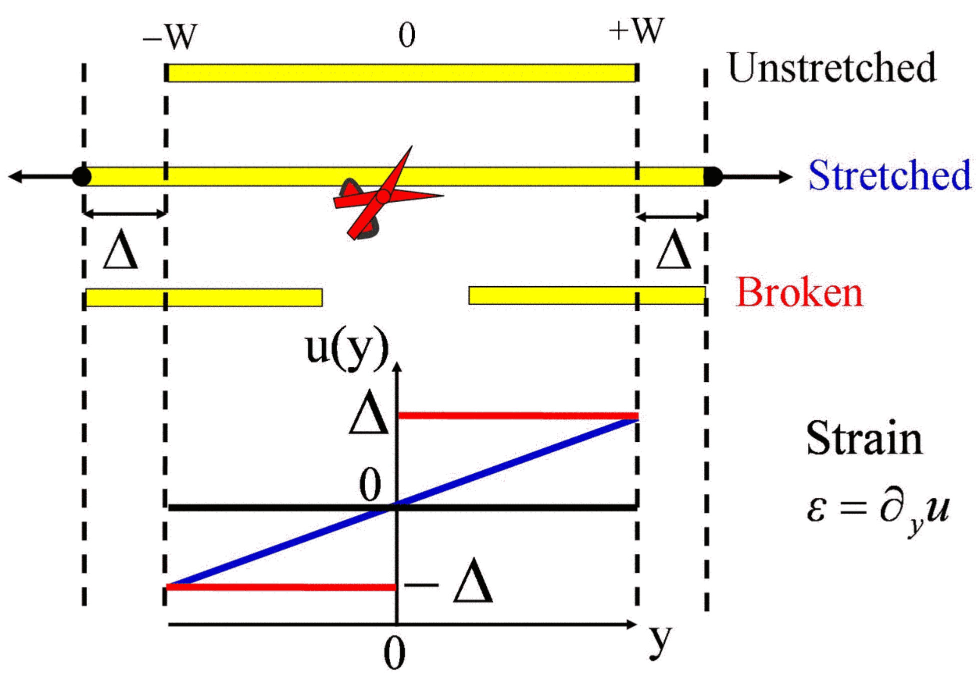

Basic idea is to "soften" the elastic energy at large strain and regularize the resulting equation with higher order derivatives.

$$E = \int dy \left[V(\varepsilon) + \frac{1}{2} g(\varepsilon)\, (\partial_y \varepsilon)^2 \right]$$

$$\text{Equilibrium}: \ \partial_y (\delta E/\delta\varepsilon) = 0$$

$$\text{Fixed displacement}: \ \int_{-W}^{W} dy\, \varepsilon = 2\Delta$$

$$\gamma = \int_0^\infty d\varepsilon \sqrt{2 g(\varepsilon) V(\varepsilon)}$$

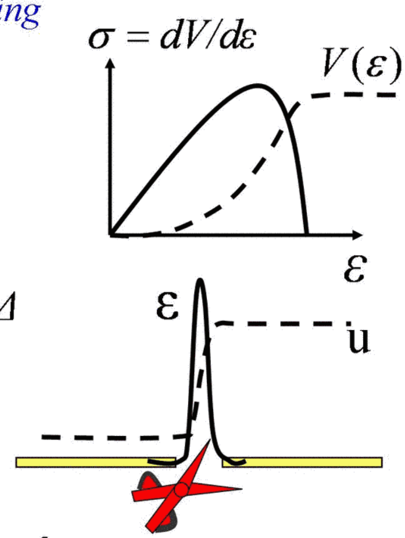

Difficulties:

(i) Fully localize the strain and obtain finite surface energy.
(ii) Yields very stiff equations with 4[th] order spatial derivatives.

V. I. Marconi and E. A. Jagla, Phys. Rev. E **71**, 036110 (2005).

Phase-Field Model

$$E = \int d\vec{x} \left[\frac{\rho}{2} \dot{u}_i^{\,2} + \frac{\kappa}{2} |\vec{\nabla}\varphi|^2 + g(\varphi)(e_{strain} - e_c) \right]$$

$$e_{strain} = \frac{\lambda}{2} u_{ii}^2 + \mu\, u_{ij}^2$$

$$u_{ij} = (\partial_i u_j + \partial_j u_i)/2$$

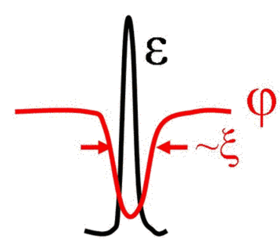

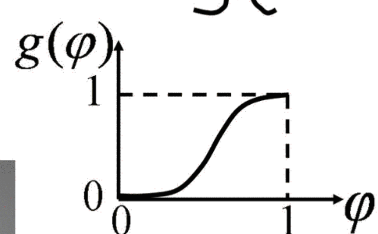

$\varphi = 1$ Normal

$\varphi = 0$ Broken

$$\dot{\varphi} = -\chi \frac{\delta E}{\delta \varphi}$$

$$\rho\, \ddot{u}_i = -\frac{\delta E}{\delta u_i}$$

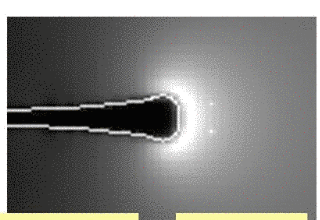

$$\xi = \sqrt{\frac{\kappa}{e_c}} \qquad \tau = \frac{1}{\chi e_c}$$

$$\gamma = e_c \xi \int_0^1 d\phi \sqrt{1 - g(\phi)}$$

A. Karma, D. Kessler, and H. Levine, Phys. Rev. Lett. **87**, 045501 (2001).

Test of local symmetry principle for anti-plane shear

Step 1: carry out phase-field (PF) simulations with time-varying displacement

$$u(x_1, x_2 = \pm W) = \pm\Delta + (A \sin \omega t) x_1$$

$\varphi(x_1,x_2)$

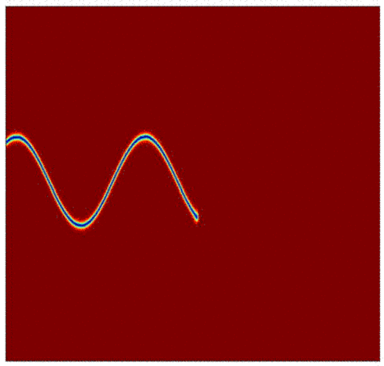

$u(x_1,x_2)$

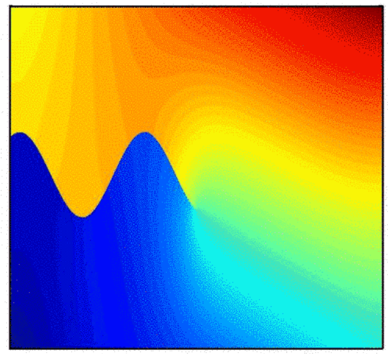

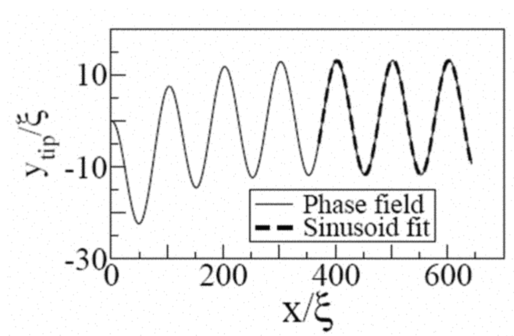

Extract from PF simulations amplitude A and phase shift ϕ of oscillations versus wavelengths λ

Step 2: compare results with analytical predictions of local symmetry principle (A_2=0) obtained by conformal mapping

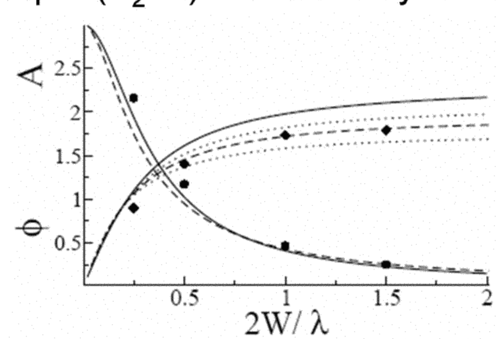

Solvability condition for the existence of crack propagating solutions on the inner scale of the process zone yields condition on K_2 (or A_2) for the outer scale standard fracture mechanics problem.

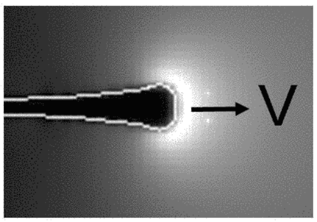

- Linearize equations of motion around stationary Griffith crack solution treating as small perturbations

$$G - G_c, K_2, A_2, \gamma_\theta$$

- Linear operator is self-adjoint and hence has zero modes corresponding to translations of the Griffith crack // and perpendicular to the crack axis

J. D. Eshelby, J. Elast. **5**, 321 (1975), and earlier references therein.

$$-\delta_{k,4} V \chi^{-1} \partial_1 \phi = \partial_j \frac{\partial \mathcal{E}}{\partial \partial_j \psi^k} - \frac{\partial \mathcal{E}}{\partial \psi^k}$$

GEM tensor:

$$T_{ij} \equiv \mathcal{E} \delta_{ij} - \frac{\partial \mathcal{E}}{\partial \partial_j \psi^k} \partial_i \psi^k$$

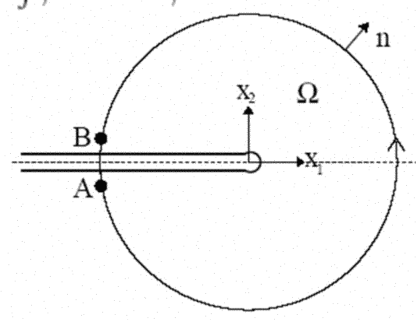

Force balance condition:

$$F_i = \int_{A \to B} ds\, T_{ij}\, n_j + \int_{B \to A} ds\, T_{ij}\, n_j - \frac{V}{\chi} \int_\Omega d\vec{x}\, \partial_1 \phi \partial_i \phi = 0$$

Configurational force | Cohesive force | Dissipative force

Force balance parallel to crack axis

$$\int_{A\to B} ds\, T_{1j}\, n_j = G \quad \text{(Rice J integral)}$$

$$\int_{B\to A} ds\, T_{1j}\, n_j = -\int_{-\infty}^{+\infty} dx_2 T_{11} = -2\gamma$$

$$F_1 \;=\; G - G_c - f_1 = 0$$

$$f_1 = V\chi^{-1}\int_{-\infty}^{+\infty}\int_{-\infty}^{+\infty} dx_1 dx_2\; (\partial_1\phi)^2$$

Force balance perpendicular to crack axis

$$\int_{B\to A} ds\, T_{2j}\, n_j = -\int_{-\infty}^{+\infty} dx_2 T_{21} = -2\gamma_\theta(0) \quad \text{(Herring torque)}$$

$$\int_{A\to B} ds\, T_{2j}\, n_j = G_\theta(0) \quad \text{(Eshelby torque)}$$

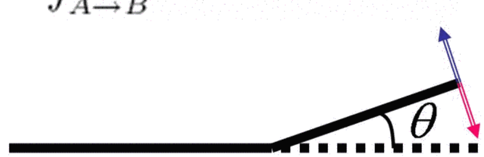

$$G_\theta(0) \;=\; -2\alpha K_1 K_2$$

$$F_2 \;=\; G_\theta(0) - G_{c\theta}(0) - f_2 = 0$$

C. Herring, *The Physics of Powder Metallurgy*, ed. by W. E. Kingston (McGraw-Hill, New York, 1951), p. 143.

M. Adda-Bedia *et al.*, Phys. Rev. E **60**, 2366 (1999)

G. E. Oleaga, J. Mech. Phys. Solids **49**, 2273 (2001)

Final result for crack path prediction

$$K_2 = -\left(G_{c\theta}(0) + f_2\right)/(2\alpha K_1)$$

$$f_2 = V\chi^{-1}\int_{-\infty}^{+\infty}\int_{-\infty}^{+\infty} dx_1 dx_2\ \partial_1\phi\partial_2\phi$$

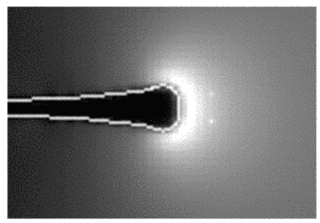

Hakim and Karma, arXiv:cond-mat/0412775 v1 31 Dec 2004

Numerical test of finite K_2 condition

$$E = \int d\vec{x}\left[\frac{\kappa}{2}|\vec{\nabla}\varphi|^2 + \varepsilon\partial_1\varphi\partial_2\varphi + g(\varphi)(e_{strain} - e_c)\right]$$

$$\gamma(\theta) = \gamma_0\sqrt{1 - (\epsilon/2)\sin 2\theta}$$

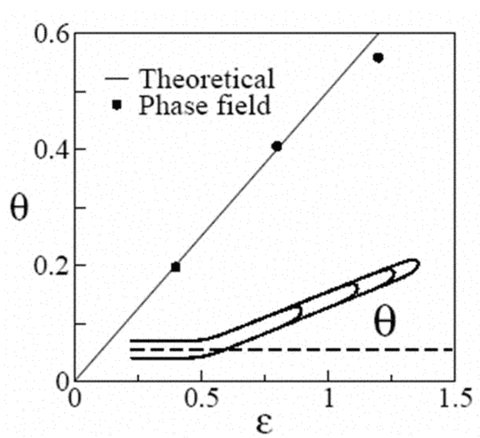

$$\theta \approx -\gamma_\theta/\gamma \approx \epsilon/2$$

When do cracks cleave crystals ?

$$\gamma(\theta) = \gamma_0(1 + \delta|\theta| + \ldots)$$

Threshold for crack to escape cleavage plane:

$$|K_2| > \frac{E\gamma_0\delta}{(1-\nu^2)K_1}$$

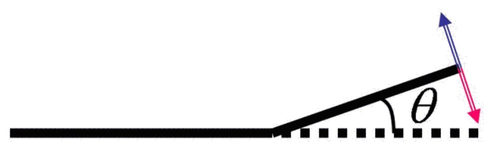

Numerical evidence for such escape threshold in lattice model:

M. Marder *Europhys. Lett.*, **66** (3), pp. 364–370 (2004)

Volume 92, Number 24 PHYSICAL REVIEW LETTERS week ending 18 JUNE 2004

Unsteady Crack Motion and Branching in a Phase-Field Model of Brittle Fracture

Alain Karma and Alexander E. Lobkovsky

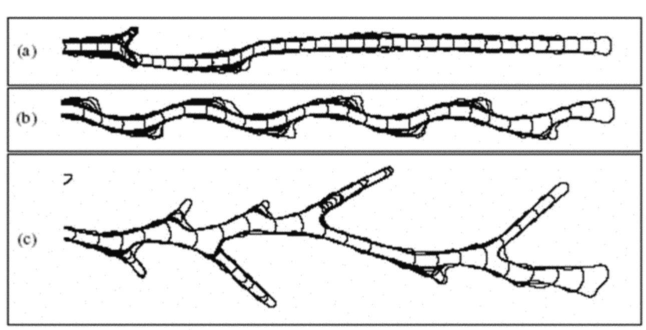

FIG. 3. Contours of $\phi = 1/2$ separated in time by $10\xi/c$. Plots are on the same scale for a strip width $W = 30\xi$, $\beta = 2$, and $\delta = 0$. (a) Transient branching for $G = 1.56G_c$. (b) Weak periodic branching (the snake) for $G = 1.86G_c$. (c) Chaotic branching for $G = 2.90G_c$.

Branching dynamics (mode III)

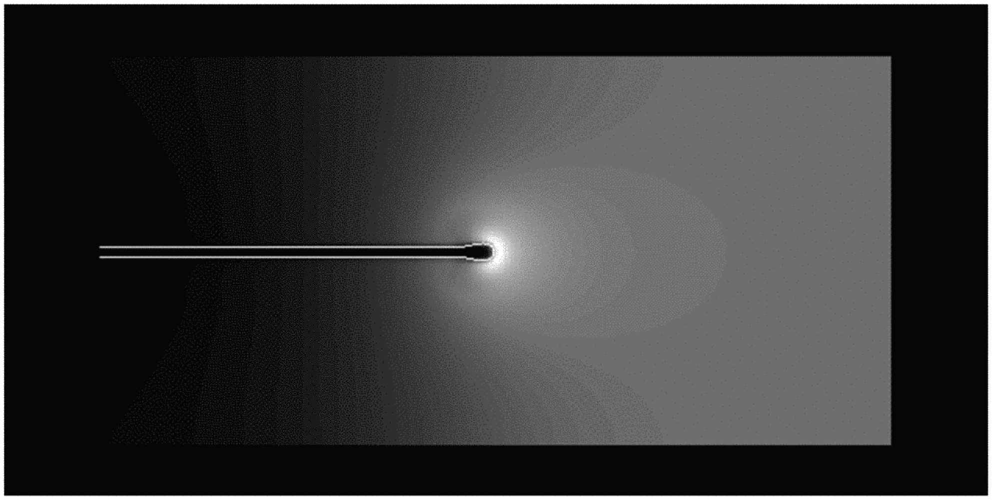

Limiting speed of crack propagation

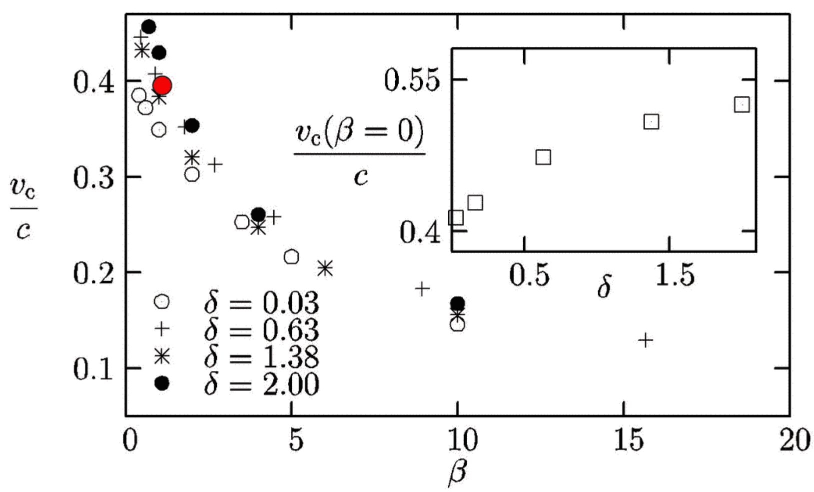

$$\beta = \frac{c\tau}{\xi}$$

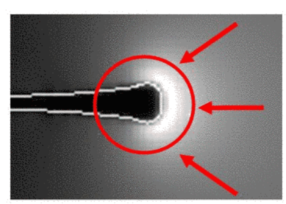

Inertia dominated

Dissipation dominated

Adda-Bedia (2002)

Maximum energy release rate → $78,4^o$ [1]

Local symmetry (A2=0) → $2\pi/5 = 72^o$

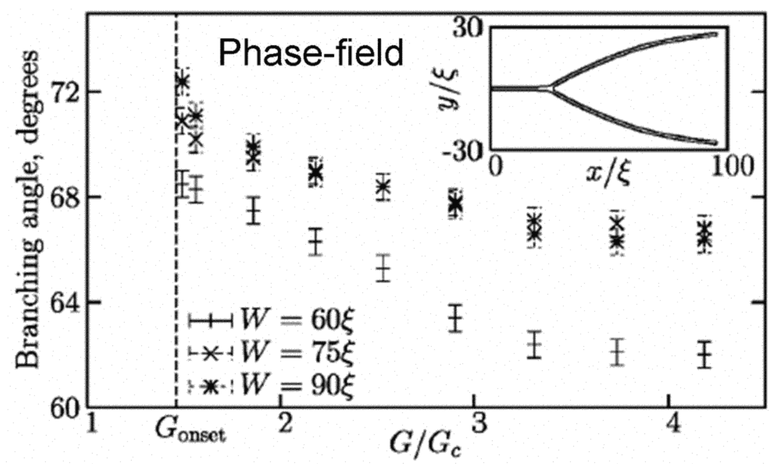

[1] M. Adda-Bedia, J. Mech. Phys. Solids **52**, 1407 (2004)

Summary

- Some clarification (we hope) of how the balance of configurational, cohesive, and dissipative forces generally determines crack paths.
- Experimentally testable condition for K_2 for anisotropic materials; existence of threshold value for propagation off cleavage plane. (New condition to our knowledge.)
- Limiting velocity and branching angle consistent with predictions from energetic bounds combined with local symmetry principle for antiplane shear. *Relatively weak effect of process zone details so far.*

Future prospects

- Incorporate asymmetry between dilation and compression (non-trivial).
- More physically motivated description of process zone (other state variables?)
- Extension to polycrystalline materials
- Extension to slip

Future prospects (continued)

- 2-d mode I for dynamic fracture
- 2-d quasi-static thermal fracture
- 3-d quasi-static fracture in mixed modes (I and III)
- 3-d dynamic fracture in mode I